Vibrational Spectroscopy and Mass Spectrometry for Characterization of Soft Landed Polyatomic Molecules

ARTICLE *in* ANALYTICAL CHEMISTRY · JUNE 2011

Impact Factor: 5.64 · DOI: 10.1021/ac200118f · Source: PubMed

3 AUTHORS, INCLUDING:

Jobin Cyriac

Indian Institute of Space Science and Techn…

21 PUBLICATIONS **225** CITATIONS

SEE PROFILE

analytical chemistry

ARTICLE

pubs.acs.org/ac

Vibrational Spectroscopy and Mass Spectrometry for Characterization of Soft Landed Polyatomic Molecules

Jobin Cyriac, Guangtao Li, and R. Graham Cooks*

Department of Chemistry, Purdue University, West Lafayette, Indiana 47907, United States

Supporting Information

ABSTRACT: We report implementation of two powerful characterization tools, in situ secondary ion mass spectrometry (SIMS) and ex situ surface enhanced Raman spectroscopy (SERS), in analyzing surfaces modified by ion soft landing (SL). Cations derived from Rhodamine 6G are soft landed onto Raman-active silver colloidal substrates and detected using SERS. Alternatively and more conveniently, high-quality SERS data are obtained by spin coating a silver colloidal solution over the modified surface once SL is complete. Well-defined SERS features are observed for Rhodamine 6G in as little as 15 min of ion deposition. Deposition of ~3 pmo1 gave high-quality SERS spectra with characteristic spectroscopic responses being derived from just ~0.5 fmol of material. Confocal SERS imaging allowed the enhancement to be followed in different parts of deposited dried droplets on surfaces. Characteristic changes in Raman spectral features occur when Rhodamine 6G is deposited under conditions that favor gas-phase ion fragmentation. Simultaneous deposition of both the intact dye and its fragment ion occurs and is confirmed by SIMS analysis. The study was extended to other Raman active surfaces, including Au nanostar and Au coated Ni nanocarpet surfaces and to SL of other molecules including fluorescein and methyl red. Overall, the results suggest that combination of SERS and SIMS measurements are effective in the characterization of surfaces produced by ion SL with significantly enhanced molecular specificity.

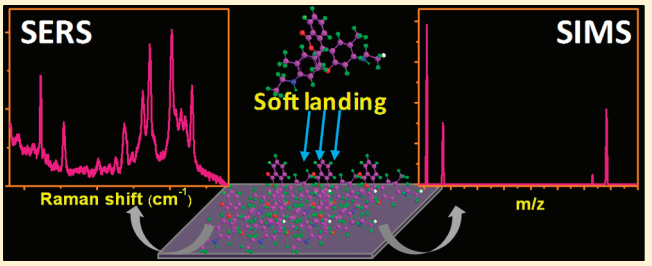

Precise knowledge and control of surface properties, especially chemical properties, is important for applications in electronics, biology, and material science. A promising method of controlled modification of surfaces is ion soft landing (SL), an experiment in which mass-selected ions of hyperthermal energy are deposited nondestructively onto a surface.[1−3] With dependence on the experimental conditions chosen and the nature of the surface and the projectile, specific chemical reactions can be implemented in the course of SL and covalent immobilization of mass selected projectiles can be achieved.[4] The uniqueness of SL compared to other methods of modification of surfaces lies in the purity of the reagents available by mass selection, the control over translational energy and the fact that the experiment is done at room temperature. In addition, it is possible to assemble complex chemical forms in the gas phase and transfer them intact onto the surface.[5] Alternative modification procedures like chemical vapor deposition (CVD), atomic layer deposition (ALD), thin film coating, etc.[6,7] are less chemically specific and less versatile but easier to implement. The disadvantages of SL include the small flux of ions available and the limited number of ways of characterizing the modified surfaces. The latter problem is addressed in this work. In particular the detection of minor amounts of compounds closely related to the main SL product is studied.

SL has been adopted for a variety of applications. These include formation of protein arrays on a substrate,[8,9] attempted preparation of catalytic surfaces,[10] cluster ion deposition,[11−13] covalent immobilization of peptides/proteins,[4,14,15] gas-phase synthesis and successive SL of organometallic compounds[5,16,17] or organic cluster ions,[18] as well as nanopatterning[19−22] among others. It has been shown that biological activity can be preserved in the course of SL of peptides like lysozyme and trypsin.[8,23,24] Digestion of cytochrome *c* using soft landed trypsin confirmed the retention of biological activity through observation of characteristic tryptic fragment of cytochrome *c* using in situ MALDI mass spectrometry (MS).[8] In another study, it was shown that the natural helical conformation of peptides was maintained during SL.[25] Singly protonated Ac-A15K was soft landed onto *N*-hydroxysuccinimidyl ester terminated alkylthiolate self-assembled monolayer surfaces (SAMs), and infrared reflection absorption spectroscopy (IRRAS) was used to identify the conformation of the soft landed species. The position and nature of the amide A and amide I and II bands clearly indicated the presence of α-helical conformation of the soft landed Ac-A15K peptide.[25]

From these studies, it is clear that postsurface characterization of soft landed material is vital in understanding its fundamentals and controlling the process to meet the needs of more demanding

Received: January 16, 2011
Accepted: May 18, 2011
Published: June 02, 2011

applications. Various in situ and ex situ studies have been used including secondary ion mass spectrometry (SIMS),[26,27] reflection absorption infrared spectroscopy (RAIRS/IRRAS/IRAS),[16,25,28] temperature programmed desorption (TPD),[16,28] surface enhanced Raman scattering/spectroscopy (SERS),[29−31] atomic force microscopy (AFM),[32] desorption electrospray ionization (DESI) MS,[33] and cyclic voltammetry (CV).[34,35] Among these, SIMS and vibrational spectroscopy have been most successful.

In situ SIMS is useful in analyzing the nature of any fragmentation or reaction which accompanies the SL event.[27,36−38] Chemical modification of soft-landed species by gas-surface interfacial reactions have been successfully monitored by in situ SIMS analysis.[27] The effect of kinetic energy upon ion deposition has been studied using ex situ SIMS analysis. In particular cases, at lower energies, <35 eV, intact deposition of polyatomic organic species was observed, but at higher energies surface-induced dissociation and fragment ion deposition predominate.[20] In general, SIMS provides a highly sensitive analysis platform for SL and just a few minutes of SL at normal MS ion currents is enough to yield good quality SIMS spectra.[27]

Structural and conformational analysis of soft-landed species can be achieved using vibrational spectroscopy. Conformation analysis of peptides using IRRAS has already been mentioned.[25] In other experiments, covalent immobilization of peptides and other organic species was achieved by reactive landing and the products were monitored using IRRAS.[4,14] The presence of amide bands in the infrared spectra confirmed successful reaction. SL has been used to isolate gas-phase generated multidecker sandwich clusters of $V_n(benzene)_{n+1}^+$ which are otherwise difficult to generate in solution phase chemistry.[5] Other simple metal sandwich clusters of M-$(benzene)_2$ were also collected by SL and analyzed using IRRAS.[28,39]

SERS[40] is the alternative spectroscopic method for analyzing soft-landed species at surfaces and it is particularly appropriate when Raman-enhancing substrates are available. SERS is highly sensitive in the case of samples on Ag nanoparticles. SL of polyatomic ions onto plasma-treated roughened Ag surfaces has been studied using SERS.[29] The detection limits can be submonolayer and a 10^5-10^6 enhancement has been reported for soft landed crystal violet. Structural studies of small carbon ($C_{1,2,4}$) or silicon ($Si_{4,6,7}$) clusters prepared by size selected SL have also been performed by SERS.[30,31]

Here, we report implementation of two powerful characterization tools; in situ SIMS and ex situ Raman spectroscopy in analyzing soft landed species. The combination of SIMS and SERS measurements helps to maximize sensitivity and chemical specificity in MS and structural and conformational information in spectroscopy. Compared to a previous report, we have achieved higher sensitivity and faster detection of soft landed species.[29] Rhodamine 6G and silver colloid coated substrates were used as model analyte and SERS system, respectively. To test the capabilities of detection of closely related species on surfaces, SERS spectra of Rhodamine 6G fragments generated by gas phase collisions were examined.

EXPERIMENTAL SECTION

Materials. Silver nitrate, Rhodamine 6G, Rhodamine B, 2′,7′-dichlorofluorescein, methyl red hydrochloride, chloroauric acid, and nickel chloride were purchased from Sigma-Aldrich (St. Louis, MO). Sodium citrate, sodium chloride, and methanol were from Mallinckrodt Chemicals (Phillipsburg, NJ). All reagents were used as received. Aqueous solutions were prepared using deionized water (18 MΩ/cm) from a Milli-Q water purification instrument (Millipore Corp., Billerica, MA). A 1:1 methanol−water solvent was used for electrospray ionization (ESI). Gold-coated (200 nm thick) silicon wafers were purchased from International Wafer Service, Inc. (Colfax, CA). The term "bare gold substrate" is used in the text to represent this wafer surface.

Preparation of Soft Landing Substrate. Colloidal Ag nanoparticles were prepared by the conventional citrate reduction method.[41] The absorption spectrum of the prepared colloidal solution was measured using a Cary 100 UV−visible spectrometer. The Ag colloid (1 mL of the) was diluted to 3 mL, and 10 μL of the diluted solution was spin coated onto the bare gold substrate to prepare the SERS surface. Spin coating was achieved using a custom-built spin coater. During coating, the substrate rotation was kept at 5500 rpm and a pneumatically assisted spray (flow rate 2 μL/min) generated by an electrospray source (without an applied voltage) was directed onto the substrate. Nitrogen gas at 80 psi pressure was used as the nebulizing gas. Optical characterization of the spin-coated substrate was done with a Leica optical microscope. Scanning electron microscopy (SEM) was performed using a FEI NOVA nanoSEM instrument.

Synthesis of star-shaped gold nanoparticles and gold-coated Ni thorn films (galvanized Ni nanocarpet) used reported procedures.[42] Characterization of these materials was done by UV−visible spectroscopy and SEM. The prepared Au nanostar particles were coated onto a bare gold substrate. Gold coating of a roughened Ni substrate was achieved by simple galvanic reduction using Au(III) chloride solution. The nickel thorn substrate was dipped into 1 mM Au(III) chloride solution for 10 min. Galvanized Ni film was then directly attached to the wafer and used as the SL substrate.

Soft Landing. Details of the SL instrument, experimental procedures, and in situ SIMS analysis have been published.[27,33,43] A schematic of this custom-built SL instrument equipped with a rectilinear ion trap (RIT) mass analyzer is given in the Supporting Information, Figure S1. Rhodamine 6G cations were generated by electrospray ionization (ESI) with methanol−water (1:1) solution containing 1×10^{-5} M Rhodamine 6G at a flow rate of 1 μL/min. Similar concentrations and solvents were used in the SL experiments in the case of dichlorofluorescein and methyl red. The atmospheric interface consists of a heated capillary followed by an ion funnel to optimize the ion current. Ions are then turned 90° using a bent square quadrupole and directed into the RIT mass analyzer using einzel lenses. The RIT serves as a mass filter for ions about to be soft landed and also as the mass analyzer during mass analysis in SIMS characterization experiments. During SL, ions exiting the RIT were focused onto the substrate by another set of einzel lenses. In a typical experiment, the ion current for Rhodamine 6G SL was 3×10^{-10} A and the average kinetic energy was measured as ∼4 eV and the spot size (estimated by optical microscopy) was 4 mm^2. In situ SIMS analysis was performed using Cs^+ ions from a primary ion source located 45° to the surface normal. The primary ion energy used for the present experiments was in the range 3−4 keV. The same RIT mass analyzer was used in the mass selective instability mode for detecting secondary ions produced in the SIMS analysis. The two different sets of voltages applied to the ion optics in normal SL experiments and fragment

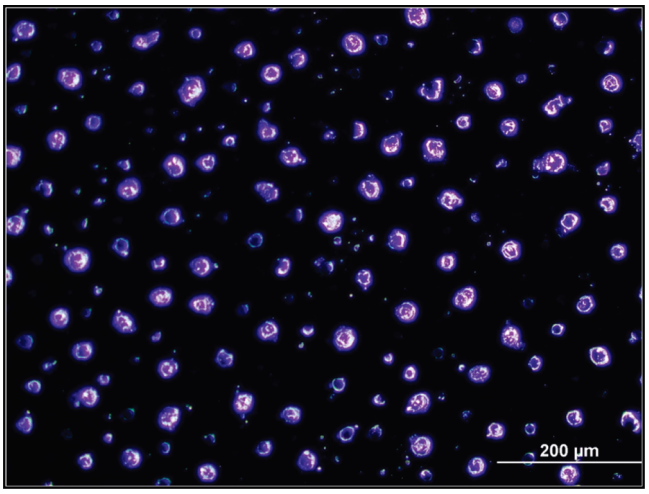

Figure 1. Dark field optical image of the substrate after spin coating the Ag citrate colloid: a 60× objective was used to record the image after spin coating the Ag colloidal solution (10 μL) onto a 1 cm × 1 cm size gold-coated silicon wafer.

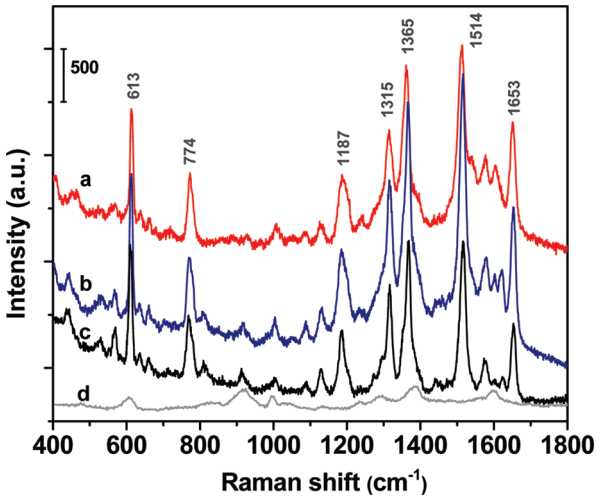

Figure 2. Raman spectra of Rhodamine 6G from various experiments (a) Rhodamine 6G soft landed onto Ag citrate coated substrate; SL current was ~3 × 10^{-10} A for 1 h. (b) Spectrum recorded after mixing Rhodamine 6G and Ag citrate colloid and spin coating 10 μL of the solution onto the bare gold substrate. The solution was prepared by mixing 1 mL of 2 × 10^{-7} M Rhodamine 6G with 1 mL of colloidal Ag. (c) Rhodamine 6G (10 μL of 1 × 10^{-7} M) directly spin coated onto a Au substrate coated with colloidal silver. (d) Ag citrate background spectrum.

deposition experiments are given in the Supporting Information, Figure S1.

Raman Spectroscopy. SERS measurements were done using a HORIBA Jobin Yvon Raman spectrometer equipped with a CCD detector and a 632.8 nm He−Ne 35 mW excitation laser source (Melles Griot). The spectra were collected using a 40× objective and 1200 lines/mm grating (unless otherwise it is mentioned), and the laser power was controlled to ~10 mW at the sample. The laser spot size was 30 μm. Acquisition time was 5 s unless otherwise mentioned. This acquisition time is much shorter than earlier SERS detection of soft landed species which required several minutes (1−60 min) exposure time.[29] All spectra are presented as collected but ordinates may be shifted to facilitate comparison. A typical experimental procedure followed the order: (i) spin coating, (ii) SL, (iii) in situ SIMS, and (iv) ex situ SERS. Substrates were removed from the SL chamber and characterized by Raman spectroscopy under ambient conditions. Rhodamine 6G solutions were prepared in 1:1 methanol−water solvent and incubated with Ag citrate colloidal solution for 5 min before spin coating onto the substrate for collecting reference spectra. Raman spectral imaging of the soft landed material was done in a Witec alpha300 confocal Raman instrument with similar He−Ne excitation laser source to that used in SERS (Melles Griot). The laser beam size for the imaging experiments was 1 μm. The substrate with soft landed material was mounted on a piezo-equipped scan stage for spectral imaging, and a 1 s acquisition time was used during imaging.

RESULTS AND DISCUSSION

The dark field optical image of silver citrate spin coated onto a SL substrate (Figure 1) shows an average droplet diameter of ~30 μm. The UV−visible absorption spectrum of the prepared Ag colloid solution and an SEM image of the spin coated colloid are given in the Supporting Information, parts A and B of Figure S2, respectively. The absorption spectrum maximum at 416 nm corresponds to ~45 nm Ag particles. The SEM image reveals that the colloid consists of particles of varying sizes and shapes. There are several aggregates present in the image, and these are assumed to assist in Raman signal enhancement. Freshly prepared spin-coated substrate worked well in contrast to substrates a few days old. Also, compared to simple drop cast surface preparations, the aggregates formed showed relatively few nanoparticles which were uniformly distributed throughout the tiny droplets formed during spin coating. Fast evaporation of solvent in spin coating helps to form a uniform distribution of less tightly packed aggregates. It should be mentioned that the laser beam and the droplet diameter were similar in size. These facts suggest that the surface prepared by spin coating makes a fairly uniform substrate for SERS.

Rhodamine 6G cations ($Rh\,6G^+$) generated by ESI were soft landed onto the Ag colloid substrate for 1 h. SL current of 3 × 10^{-10} A, viz., ~6.7 × 10^{12} ions were deposited onto the substrate in an area of 1 cm × 1 cm. The corresponding SERS spectrum (Figure 2a) shows all the Raman features known to correspond to Rhodamine 6G. Peak assignments are based on earlier reports:[44,45] peaks at 613, 774, and 1187 cm^{-1} are associated with C−C−C ring in-plane, C−H out-of-plane bending (or in-plane deformation of xanthenes ring[45]) and C−C stretching vibrations, respectively. Bands at 1315, 1365, 1514, and 1653 cm^{-1} are assigned to aromatic C−C stretching vibrations of Rhodamine 6G molecules. These vibrational frequencies and relative spectral intensities are similar (within a few cm^{-1}) to the reported SERS of Rhodamine 6G. Two reference SERS spectra were recorded to compare Raman features of the soft landed species. One of them was prepared by mixing 1 mL of 2 × 10^{-6} M Rhodamine 6G solution in water−methanol (1:1) with 1 mL of Ag citrate solution. This mixture was incubated for 5 min, and 10 μL of the sample was then spin coated onto the bare gold substrate for SERS measurements. The second sample was prepared by spin coating 10 μL of Ag colloid onto the bare gold substrate followed by coating 10 μL of 1 × 10^{-6} M Rhodamine 6G over it. Both samples were coated onto an area of ~1 cm × 1 cm. The number of analyte molecules present in the reference

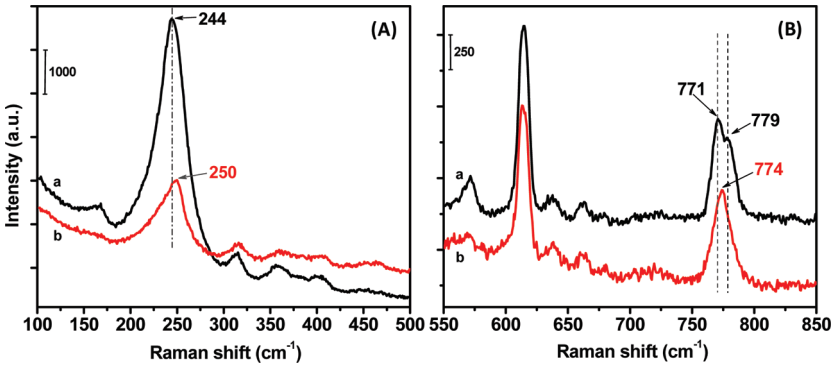

Figure 3. Raman features in shorter wavelength region (A) Peak corresponding to Ag−N is blue-shifted in the case of soft landed Rhodamine 6G. Spectrum A(a) is for Rhodamine 6G prepared by spin coating and A(b) is obtained by SL. (B) The peak due to C−H out-of-plane bending at ∼775 cm^{-1} is split in the presence of Cl^- anions when the sample is spin-coated, (B(a)), but the vibration is degenerate when the dye is soft landed (B(b)).

experiment was comparable to that in the SL experiment. The intensities and positions of the spectral bands of the reference samples were similar to those of the soft landed species as shown in Figure 2b,c.

The nearly planar xanthene moiety is responsible for most of the vibrational features of Rhodamine 6G just noted.[45,46] It has been reported that this part of the molecule lies flat on the Ag surface.[44] The intact features suggest that Rhodamine 6G neither undergoes chemical reactions nor conformational changes in the course of SL deposition.

A remarkable observation was made relative to differences in analyte−metal interaction occurring upon SL. Although the wavelength region shown in Figure 2 does not demonstrate any apparent difference between the materials generated by deposition by SL and solution coating, the shorter wavelength regime does show differences (Figure 3). The band around 240 cm^{-1} corresponding to the Ag−N stretching vibration results from the interaction between the ethylamino group of Rhodamine 6G and Ag.[44] Raman spectra of nitrogen-containing compounds adsorbed on Ag show spectral bands at this position suggesting that this feature is mainly due to chemisorption through the N atom.[47] In the present case, this band was observed at 244 cm^{-1} for solution coated samples and at 250 cm^{-1} for those produced by SL (Figure 3A). The band due to Ag−N complexation is blue-shifted by 6 cm^{-1} for soft landed Rhodamine 6G, suggesting that the Ag−N interaction is stronger for soft landed species. Most likely the absence of a deposited anion plays an important role here. The argument is further supported by the band degeneracy in the 774 cm^{-1} feature for soft landed Rhodamine 6G (Figure 3B). The band at ∼775 cm^{-1} is attributed to the C−H out-of-plane bending mode.[44] This band was split into two in the solution coated sample. In the solution-phase coating, the Cl^- anion is closely associated with the Rhodamine cation but for SL only the cation was landed onto the substrate. Hence, the formation of the Ag−Rhodamine 6G complex can be degenerate in the SL method as both rings of Rhodamine 6G can interact with the metal in a similar way.[44] In the presence of Cl^-, the rings interact differently which splits the band due to C−H out-of-plane bending. It is noteworthy that full-width at half-maximum (fwhm) of this peak increased from 16 to 20 cm^{-1} in the presence of chloride. The observations suggest that the subtle changes in molecular conformations in SL can be accessed by SERS analysis.

Control experiments have been performed to establish the sensitivity of SERS in postsurface analysis. SL for 15 min duration produced reasonable Raman signal for Rhodamine 6G (Figure 4A). All the bands observed with the 1 h SL experiment were clearly distinguishable in this short deposition case as well. The 3×10^{-10} A ion current landed approximately 1.7×10^{12} molecules on the surface in 15 min. Considering the spot size of 7×10^{-10} m^2 that was irradiated by the laser and assuming uniform distribution of analyte molecules on the surface, the number of molecules causing the spectroscopic response is equivalent to ∼0.5 fmol. It should be noted that the total amount of the soft landed Rhodamine 6G is much higher, ∼3 pmol.

Instead of SL onto a special SERS active surface, SERS of soft landed species could be recorded by spin coating Ag colloids after SL is complete. This facilitates use of SL for chemical modification of surfaces in general, independently of considerations of the characterization methodology. Pronounced Raman signal enhancement was observed compared to SL Rhodamine 6G onto a Ag colloid coated substrate. Figure 4B(a) shows that Raman spectrum of Rhodamine 6G soft landed onto bare gold substrate followed by spin coating Ag colloidal solution. The duration and current of SL was 1 h and 3×10^{-10} A, respectively, which was identical to the previous experiments. A SERS spectrum collected in the normal procedure is given as Figure 4B(b). Spin coating followed by SL results in ∼6-fold signal enhancement compared to deposition onto a SERS active substrate. The spectrum recorded after SL of Rhodamine 6G onto a bare gold substrate did not give a Raman response (Figure 4B(c)).

Use of a confocal Raman instrument allowed high spatial resolution examination of the signal response from soft landed Rhodamine 6G species across individual Ag colloid droplets. A Raman spectral image of the soft landed substrate is given in the Supporting Information, Figure S3B, and the corresponding optical image is given as Figure S3A in the Supporting Information. In these imaging measurements, the spot size at the laser irradiation site was ∼1 μm, which is much smaller than in the previous experiments. Therefore, the spectral image can provide fine details of a single droplet. Images for the region 1550−1660 cm^{-1} make it obvious that the signal intensity was higher where the Ag aggregates or Ag particle density is higher, especially at the circumference of circular drops formed in spin coating. Images corresponding to other wavenumber regions were also examined thoroughly. Intensity variations occurred, but no spectral band shift was observed across the imaged area. This further supports the hypothesis that soft landed Rhodamine

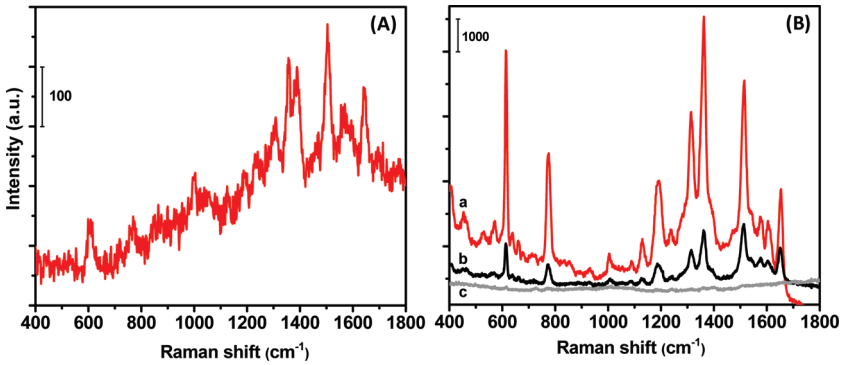

Figure 4. (A) SERS spectrum of Rhodamine 6G soft landed for 15 min. (B) Signal enhancement observed when Ag colloid was spin-coated over Rhodamine 6G previously soft landed on a bare gold substrate. (B) Part a shows Raman spectra after spin coating Ag citrate onto soft landed Rhodamine 6G, and part c represents the spectrum recorded before the Ag citrate coating step. The spectrum in part b is given for reference; it shows Rhodamine 6G soft landed onto the Ag citrate substrate using the normal conditions.

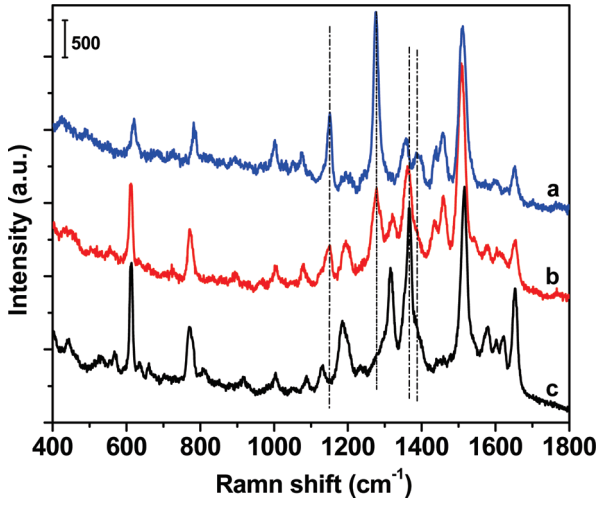

Figure 5. Rhodamine 6G soft landed under different experimental conditions (traces b and c): Spectrum a represents the SERS spectrum of soft landed Rhodamine B under normal conditions (given for comparison). Spectrum b represents SERS spectrum of Rhodamine 6G in conditions favorable for fragmentation and spectrum c is normal SL conditions. Two distinct features at 1150 and 1279 cm^{-1} clearly indicate the contributions of fragments in the soft landed species.

6G ions did not undergo any reaction other than chemisorption or conformational changes in the course of SL.

The selection of available SERS substrates is broad. Several other Raman active substrate were used to further demonstrate that SERS is a very useful tool in analysis of surfaces prepared by SL. Au nanostar coated substrate and galvanized Ni nanocarpet surface were two other substrates selected. The Raman responses and corresponding SEM images for these two substrates are given in Supporting Information, Figure S4.The Raman features were more or less identical except for 1−2 cm^{-1} shifts in some cases which cannot be attributed to any substantial molecular changes. Among the three substrates used, Ag colloid substrate was best in sensitivity and spectral quality. Other differences such as those in the metal−Rhodamine 6G interactions were not clearly distinguishable for gold nanostar and galvanized Ni nanocarpet substrates.

SERS characterization of Rhodamine 6G fragment ion SL as minor components in an ionic mixture including the intact

Scheme 1. (a) Structure of Rhodamine 6G Cation and Possible Fragmentation (b) Structure of Rhodamine B Cation

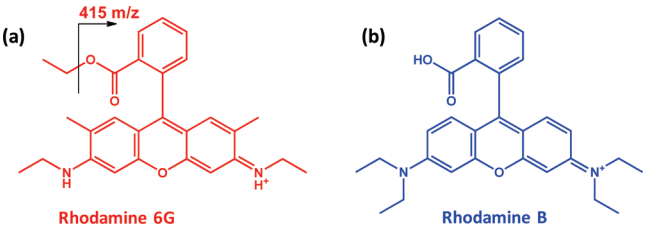

cations was examined to determine molecular specificity of the analytical methods (SIMS and SERS) used here. Changes were made in experimental conditions (Supporting Information, Figure S1) to favor gas phase fragmentation of Rhodamine 6G. As the potential difference between the skimmer and the lens 1 of the einzel lens was increased to >15 V, postsource fragmentation due to collisions with background gas occurred and these fragments were deposited onto the substrate.[48,49] The SERS spectra given in Figure 5b,c represent Rhodamine 6G soft landed under conditions favorable to postsource fragmentation and normal conditions, respectively. The additional features at 1150 and 1277 cm^{-1} appear to be due to a different molecular species. In addition, intensity differences for the features at 1187, 1315, and 1367 cm^{-1} are also observed. The probable fragmentation of Rhodamine 6G at the C−O bond position is illustrated in Scheme 1a. The existence of this fragment was confirmed in two different ways. First, in situ SIMS analysis was utilized to identify the excess fragment at the surface. The increased intensity of m/z 415 in the product ion spectrum compared to soft landed Rhodamine 6G using normal settings (parts A and B of Figure 6, respectively) clearly supports deposition of the fragment ion. SIMS fluxes were kept at static limits to reduce the primary ion induced fragmentation. Fragment ion formation and deposition was further confirmed by mass spectral analysis. When the mass analyzer was operated in the mass analysis mode with the lens and skimmer voltages favorable for fragmentation, the resulting mass spectrum consisted of an intense peak at m/z 415 which was negligible using normal SL parameters. Mass spectra corresponding to the two operating modes are given in the Supporting Information, Figure S5. Additional spectroscopic support for the deposition of fragment ions was gathered from

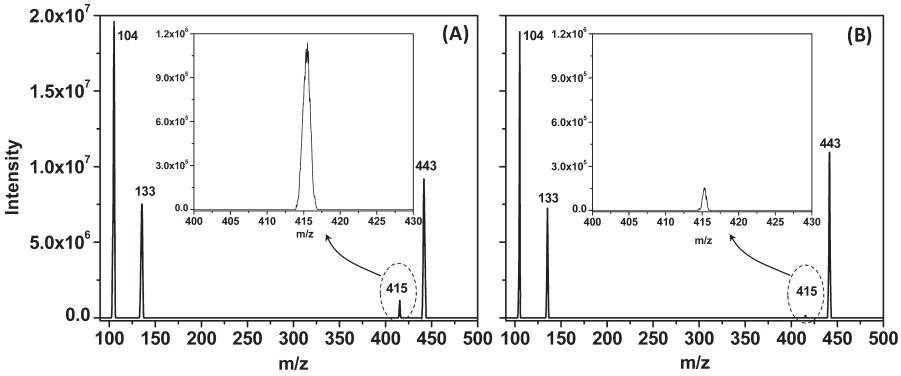

Figure 6. In situ SIMS showing the fragments generated and deposited in SL. In situ SIMS spectrum of soft landed Rhodamine 6G (A) using conditions favorable to fragmentation and (B) using normal experimental conditions. Insets in both figures show the expanded views of the m/z 415 region. The intensity of the fragment at m/z 415 in part A is ~10 times higher than in part B.

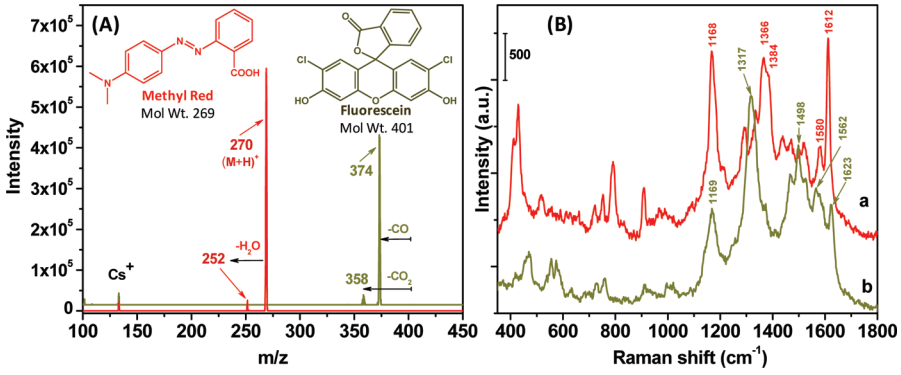

Figure 7. (A) In situ SIMS spectra of soft landed methyl red (red trace) and fluorescein (ochre trace). Protonated molecule and fragment ions formed by the loss of CO are the base peaks for the surfaces prepared by SL methyl red and fluorescein species, respectively. (B) SERS spectra collected from the soft landed methyl red (a) and fluorescein (b) species.

Raman analysis of a compound with a chemical structure similar to that of the fragment. The fragment shares a structural similarity with Rhodamine B molecule in its carbonyl side chain (Scheme 1b). The moiety formed by fragmentation has the same xanthene backbone as does Rhodamine 6G, but the side chain contains a carbonyl group (carboxylic) similar to the another dye, Rhodamine B. Interestingly, the features at 1152 and 1275 cm^{-1} were observed for SERS of Rhodamine B soft landed onto the same substrate using normal SL conditions (Figure 5a). These facts support the argument that the fragment is formed by C−O bond dissociation in the ethoxy side chain. In addition, a 20:80 mixture of Rhodamine B and Rhodamine 6G resulted in the similar SERS features to those in the fragment containing SERS which is given in Figure 5b. The spectroscopic and mass spectral information confirm that SERS and SIMS can be used to detect small amounts of SL compounds that are closely related to the main SL species.

The SERS and in situ SIMS characterization methodology has been extended to the characterization of surfaces prepared by SL of methyl red and dichlorofluorescein species onto Raman active Ag colloidal substrates. Similar to the experiments described, protonated methyl red molecules generated by ESI were soft landed onto the Ag colloidal substrate for 1 h (SL current was ~2 × 10^{-10} A). The in situ SIMS spectrum (Figure 7A(a)) contains species due to the desorption of methyl red as the protonated ion, and its gas-phase fragment by loss of H_2O confirms successful SL. The SERS spectrum of the soft landed species (Figure 7B(a)) shows identical Raman features to that of a reference sample prepared by mixing of 1 mL of Ag nanoparticle and 1 mL of 2 × 10^{-6} M methyl red solution in water−methanol (1:1) further supporting the SL event. The important Raman features present in the SERS spectrum were assigned based on earlier literature.[50−52] The strong band at 1612 cm^{-1} is due to C═C and C═N vibration of the quinonoid ring.[51] The bands at 1580, 1384, and 1366 cm^{-1} are attributed to ν(C-ring), N═N, and unresolved in-plane C−H/N−C(ring) vibrations, respectively. The strong band at 1168 cm^{-1} could be unresolved δ(in-plane (CH)(C-ring), δC−OH vibrations. Interestingly, for the case of fluorescein SL, in situ SIMS did not produce intact molecular ions. The major peaks in the spectrum (Figure 7A(b)) are assigned to the loss of CO and CO_2 species from the protonated fluorescein molecule. It should be noted that the resolving power of the mass spectrometer was not adequate to show the chlorine isotopic pattern and the peaks are assigned to nominal mass. Figure 7B(b) illustrates the SERS spectrum of soft landed fluorescein species. SL was performed for 1 h at ~2 × 10^{-10} A current. The features appeared at 1623, 1562, and 1317 cm^{-1} are assigned to C−C stretching vibration from the xanthenes ring according to the earlier reports.[53,54] Other major features were observed at 1498 cm^{-1} (central ring breathing) and 1169 cm^{-1} (CCH bend on xanthenes ring). The absence of fluorescein molecular species in the SIMS spectrum may be misleading by suggesting that a

dx.doi.org/10.1021/ac200118f |*Anal. Chem.* 2011, 83, 5114–5121

fragment ion has been deposited. However, the comparison of SERS spectra of soft landed species and that of the reference experiment (Supporting Information, Figure S6) suggest the presence of intact fluorescein molecule at the surface. As in the other cases, the reference spectrum was collected from the surface prepared by spin coating a mixture of 1 mL of 2×10^{-6} M fluorescein solution in water−methanol (1:1) with 1 mL of Ag citrate solution. Moreover, fluorescein coated bare Au substrate results in similar SIMS spectrum support that SL occurred. These sets of SL experiments demonstrate that the observation from the complementary methods of in situ SIMS/ex situ SERS characterize the soft landed species.

CONCLUSIONS

We have demonstrated that SERS is a powerful tool for analysis of surface modifications made by SL. Reproducible SERS features with good signal-to-noise ratio were obtained even from 15 min of SL. The Raman spectra of soft landed Rhodamine 6G species and the systems prepared by solution-phase incubation provide similar features suggesting that SL under normal conditions does not cause fragmentation or change the molecular structure. Raman spectroscopy revealed intact SL and distinguished these species from SL of a gas-phase dissociation product. Distinctive Raman features were observed for the deposited fragments compared to the intact molecules. The study is noteworthy for demonstrating that SL leads to differences in metal−analyte species interaction compared to solution phase deposition of the same molecules. The complementary combination of SERS and in situ SIMS is capable of providing the necessary spectroscopic information and chemical specificity of the soft landed species and for recognizing fragmentation and other chemical changes in the course of SL. It should be noted that in such experiments the choice of Raman active substrate, a deliberately nonconducting surface, is critical. The fact that the SERS active substrate can be added after SL is complete increases the value of these methods.

The novelty of the present paper lies in these facts: (i) the implementation of SERS and SIMS to study SL surfaces, (ii) the demonstration of complementarity to study features that might give subtle effects in one case (e.g., structural changes recognized in C−H out-of-plane bending in SERS but not evident in SIMS) or the other (e.g., fragmentation seen in SIMS but causing small effects in SERS), (iii) in the 10-fold increased sensitivity (5 s acquisition time, 15 min SL) compared to earlier SL experiments, (iv) in the simplicity of the SERS system including ease of preparation of the Ag colloid, (iv) its addition on top of the modified surface, (v) the use of imaging confocal SERS to characterize the soft landed species, and finally (vi) the identification of two closely related structural species at the surface.

ASSOCIATED CONTENT

Supporting Information. Additional information as noted in text. This material is available free of charge via the Internet at http://pubs.acs.org.

AUTHOR INFORMATION

Corresponding Author

*E-mail: cooks@purdue.edu. Address: R. Graham Cooks, Department of Chemistry, Purdue University, West Lafayette, IN 47907.

ACKNOWLEDGMENT

This work was supported by U.S. Department of Energy Grant DE-FG02-06ER15807 and Thermo Fisher Scientific for instrumentation. The authors thank Dr. Alexander E. Ribbe for the confocal Raman image and Mr. Jason Duncan for help with electronics.

REFERENCES

(1) Miller, S. A.; Luo, H.; Pachuta, S. J.; Cooks, R. G. *Science* **1997**, *275*, 1447–1450.
(2) Grill, V.; Shen, J.; Evans, C.; Cooks, R. G. *Rev. Sci. Instrum.* **2001**, *72*, 3149–3179.
(3) Laskin, J.; Wang, P.; Hadjar, O. *Phys. Chem. Chem. Phys.* **2008**, *10*, 1079–1090.
(4) Wang, P.; Hadjar, O.; Laskin, J. *J. Am. Chem. Soc.* **2007**, *129*, 8682–8683.
(5) Nagaoka, S.; Matsumoto, T.; Ikemoto, K.; Mitsui, M.; Nakajima, A. *J. Am. Chem. Soc.* **2007**, *129*, 1528–1529.
(6) George, S. M. *Chem. Rev.* **2010**, *110*, 111–131.
(7) Serp, P.; Kalck, P.; Feurer, R. *Chem. Rev.* **2002**, *102*, 3085–3128.
(8) Ouyang, Z.; Takats, Z.; Blake, T. A.; Gologan, B.; Guymon, A. J.; Wiseman, J. M.; Oliver, J. C.; Davisson, V. J.; Cooks, R. G. *Science* **2003**, *301*, 1351–1354.
(9) Blake, T. A.; Zheng, O. Y.; Wiseman, J. M.; Takats, Z.; Guymon, A. J.; Kothari, S.; Cooks, R. G. *Anal. Chem.* **2004**, *76*, 6293–6305.
(10) Peng, W. P.; Johnson, G. E.; Fortmeyer, I. C.; Wang, P.; Hadjar, O.; Cooks, R. G.; Laskin, J. *Phys. Chem. Chem. Phys.* **2011**, *13*, 267–275.
(11) Vajda, S.; Pellin, M. J.; Greeley, J. P.; Marshall, C. L.; Curtiss, L. A.; Ballentine, G. A.; Elam, J. W.; Catillon-Mucherie, S.; Redfern, P. C.; Mehmood, F.; Zapol, P. *Nat. Mater.* **2009**, *8*, 213–216.
(12) Lei, Y.; Mehmood, F.; Lee, S.; Greeley, J.; Lee, B.; Seifert, S.; Winans, R. E.; Elam, J. W.; Meyer, R. J.; Redfern, P. C.; Teschner, D.; Schlogl, R.; Pellin, M. J.; Curtiss, L. A.; Vajda, S. *Science* **2010**, *328*, 224–228.
(13) Kaden, W. E.; Wu, T. P.; Kunkel, W. A.; Anderson, S. L. *Science* **2009**, *326*, 826–829.
(14) Hu, Q. C.; Wang, P.; Gassman, P. L.; Laskin, J. *Anal. Chem.* **2009**, *81*, 7302–7308.
(15) Wang, P.; Hadjar, O.; Gassman, P. L.; Laskin, J. *Phys. Chem. Chem. Phys.* **2008**, *10*, 1512–1522.
(16) Ikemoto, K.; Nagaoka, S.; Matsumoto, T.; Mitsui, M.; Nakajima, A. *J. Phys. Chem. C* **2009**, *113*, 4476–4482.
(17) Peng, W. P.; Goodwin, M. P.; Chen, H.; Cooks, R. G.; Wilker, J. *Rapid Commun. Mass Spectrom.* **2008**, *22*, 3540–3548.
(18) Nanita, S. C.; Takats, Z.; Cooks, R. G. *J. Am. Soc. Mass Spectrom.* **2004**, *15*, 1360–1365.
(19) Rader, H. J.; Rouhanipour, A.; Talarico, A. M.; Palermo, V.; Samori, P.; Mullen, K. *Nat. Mater.* **2006**, *5*, 276–280.
(20) Rauschenbach, S.; Vogelgesang, R.; Malinowski, N.; Gerlach, J. W.; Benyoucef, M.; Costantini, G.; Deng, Z. T.; Thontasen, N.; Kern, K. *ACS Nano* **2009**, *3*, 2901–2910.
(21) Rouhanipour, A.; Roy, M.; Feng, X. L.; Rader, H. J.; Mullen, K. *Angew. Chem., Int. Ed.* **2009**, *48*, 4602–4604.
(22) Thontasen, N.; Levita, G.; Malinowski, N.; Deng, Z.; Rauschenbach, S.; Kern, K. *J. Phys. Chem. C* **2010**, *114*, 17768–17772.
(23) Gologan, B.; Takats, Z.; Alvarez, J.; Wiseman, J. M.; Talaty, N.; Ouyang, Z.; Cooks, R. G. *J. Am. Soc. Mass Spectrom.* **2004**, *15*, 1874–1884.
(24) Volny, M.; Elam, W. T.; Ratner, B. D.; Turecek, F. *Anal. Chem.* **2005**, *77*, 4846–4853.
(25) Wang, P.; Laskin, J. *Angew. Chem., Int. Ed.* **2008**, *47*, 6678–6680.
(26) Johnson, G. E.; Lysonski, M.; Laskin, J. *Anal. Chem.* **2010**, *82*, 5718–5727.
(27) Nie, Z. X.; Li, G. T.; Goodwin, M. P.; Gao, L.; Cyriac, J.; Cooks, R. G. *J. Am. Soc. Mass Spectrom.* **2009**, *20*, 949–956.
(28) Nagaoka, S.; Ikemoto, K.; Matsumoto, T.; Mitsui, M.; Nakajima, A. *J. Phys. Chem. C* **2008**, *112*, 15824–15831.

(29) Volny, M.; Sengupta, A.; Wilson, C. B.; Swanson, B. D.; Davis, E. J.; Turecek, F. *Anal. Chem.* **2007**, *79*, 4543–4551.
(30) Haslett, T. L.; Fedrigo, S.; Moskovits, M. *J. Chem. Phys.* **1995**, *103*, 7815–7819.
(31) Honea, E. C.; Ogura, A.; Murray, C. A.; Raghavachari, K.; Sprenger, W. O.; Jarrold, M. F.; Brown, W. L. *Nature* **1993**, *366*, 42–44.
(32) Duffe, S.; Gronhagen, N.; Patryarcha, L.; Sieben, B.; Yin, C. R.; von Issendorff, B.; Moseler, M.; Hovel, H. *Nat. Nanotechnol.* **2010**, *5*, 335–339.
(33) Peng, W. P.; Goodwin, M. P.; Nie, Z. X.; Volny, M.; Zheng, O. Y.; Cooks, R. G. *Anal. Chem.* **2008**, *80*, 6640–6649.
(34) Mazzei, F.; Favero, G.; Frasconi, M.; Tata, A.; Tuccitto, N.; Licciardello, A.; Pepi, F. *Anal. Chem.* **2008**, *80*, 5937–5944.
(35) Pepi, F.; Ricci, A.; Tata, A.; Favero, G.; Frasconi, M.; Noci, S. D.; Mazzei, F. *Chem. Commun.* **2007**, 3494–3496.
(36) Hadjar, O.; Futrell, J. H.; Laskin, J. *J. Phys. Chem. C* **2007**, *111*, 18220–18225.
(37) Laskin, J.; Wang, P.; Hadjar, O. *J. Phys. Chem. C* **2010**, *114*, 5305–5311.
(38) Laskin, J.; Wang, P.; Hadjar, O.; Futrell, J. H.; Alvarez, J.; Cooks, Z. G. *Int. J. Mass Spectrom.* **2007**, *265*, 237–243.
(39) Nagaoka, S.; Matsumoto, T.; Okada, E.; Mitsui, M.; Nakajima, A. *J. Phys. Chem. B* **2006**, *110*, 16008–16017.
(40) Dieringer, J. A.; Wustholz, K. L.; Masiello, D. J.; Camden, J. P.; Kleinman, S. L.; Schatz, G. C.; Van Duyne, R. P. *J. Am. Chem. Soc.* **2009**, *131*, 849–854.
(41) Kamat, P. V.; Flumiani, M.; Hartland, G. V. *J. Phys. Chem. B* **1998**, *102*, 3123–3128.
(42) Sajanlal, P. R.; Pradeep, T. *J. Phys. Chem. C* **2010**, *114*, 16051–16059.
(43) Li, G.; Cyriac, J.; Gao, L.; Cooks, R. G. *Surf. Interface Anal.* 2011, *43* (1−2), 498–501.
(44) Hildebrandt, P.; Stockburger, M. *J. Phys. Chem.* **1984**, *88*, 5935–5944.
(45) Watanabe, H.; Hayazawa, N.; Inouye, Y.; Kawata, S. *J. Phys. Chem. B* **2005**, *109*, 5012–5020.
(46) Le Ru, E. C.; Blackie, E.; Meyer, M.; Etchegoin, P. G. *J. Phys. Chem. C* **2007**, *111*, 13794–13803.
(47) Venkatesan, S.; Erdheim, G.; Lombardi, J. R.; Birke, R. L. *Surf. Sci.* **1980**, *101*, 387–398.
(48) Schneider, B. S.; Douglas, D. J.; Chan, D. D. Y. *Rapid Commun. Mass Spectrom.* **2001**, *15*, 249–257.
(49) Gao, L.; Li, G. T.; Cooks, R. G. *J. Am. Soc. Mass Spectrom.* **2010**, *21*, 209–214.
(50) Bell, S.; Bisset, A.; Dines, T. J. *J. Raman Spectrosc.* **1998**, *29*, 447–462.
(51) Bisset, A.; Dines, T. J. *J. Chem. Soc., Faraday Trans.* **1995**, *91*, 499–505.
(52) Mullen, K. I.; Wang, D. X.; Crane, L. G.; Carron, K. T. *Anal. Chem.* **1992**, *64*, 930–936.
(53) Hildebrandt, P.; Stockburger, M. *J. Raman Spectrosc.* **1986**, *17*, 55–58.
(54) Wang, L. L.; Roitberg, A.; Meuse, C.; Gaigalas, A. K. *Spectrochim. Acta, Part A: Mol. Biomol. Spectrosc.* **2001**, *57*, 1781–1791.